nzsee
NEW ZEALAND SOCIETY FOR EARTHQUAKE ENGINEERING

Predictive models for changes in reinforcement characteristics due to strain ageing effects

A.V. Shegay, K. Okamura & D. Sato
Tokyo Institute of Technology, Yokohama, Japan.

ABSTRACT

One of the factors affecting repair feasibility of buildings damaged by earthquakes is the potential effects of strain ageing of reinforcement. Since strain ageing can lead to an increase in structural member strength and ductility reduction, the strength hierarchy set through capacity design disruptions can be disrupted leading unexpected seismic response of individual members or the structure as a whole. In this study, characteristics of reinforcement strain ageing were investigated through testing of several grades of reinforcement under a range of loading and ageing conditions. It was found that the expected maximum increase in strength and decrease in ductility due to strain ageing can be reasonably predicted using a linear relationship with vanadium content. On the other hand, percentage of carbon was not found to have an obvious correlation. It was also found that the final strain aged reinforcement characteristics were independent of the initially applied level of strain provided that the maximum initial reinforcement response had entered the strain hardening region. Under these conditions it was also shown that the temporal change of reinforcement properties due to strain ageing could be reliably modelled via a logarithmic function.

1 INTRODUCTION

Repair of buildings damaged in earthquakes is becoming a more feasible recovery strategy given a recent advance in understanding of effects of repair on structural performance. In reinforced concrete (RC) buildings, strain ageing of reinforcement is one particular aspect that is potentially critical in considering the adverse effects of repair. As shown in Figure 1, strain ageing is a phenomenon by which yielded reinforcement will experience an increase in yield strength ($\Delta\sigma_{ya}$), increase in ultimate tensile stress ($\Delta\sigma_{ua}$) and decrease in fracture strain ($\Delta\varepsilon_{sua}$) over time, among other changes. There are two primary concerns for the potential detrimental impact these changes can have on the structure:

1) Reduction in member ductility due fracture of reinforcement at smaller strains than expected strains, and
2) A change in failure mode characteristics due to a higher-than-expected reinforcement strength.

The latter is a concern that can manifest at the member level (e.g., structural wall transition from a flexural failure to a shear failure, or reinforcement bond failure) as well as at the system level (e.g., columns yielding before beams in a moment frame). The strain ageing phenomena has been experimentally observed in several studies on the repair of RC members (Mikawa et al., 2022; Nagai et al., 2022; Sarrafzadeh, 2021; Tasai, 1988) and structures (Shegay et al., 2023).

Research specifically into strain ageing effects on reinforcement has been particularly well researched in New Zealand (Loporcaro, 2017; Momtahan et al., 2009; Pussegoda, 1978). These studies have shown that the G300E reinforcement is susceptible to strain ageing effects while G500 is not. The main element distinguishing the reinforcement susceptibility to strain ageing was the differing vanadium content (present as an additive to enhance reinforcement elongation properties). Because these studies have focused on testing different 'grades' of reinforcement, the results of these studies are not easily applicable to reinforcement grades available in other countries. As a result, the studies did not reach a stage where a generalized model was proposed to enable prediction of not only susceptibility of a given reinforcement grade to strain ageing, but also the magnitude its effects. Therefore, the objective of this study was to identify the factors that influence the susceptibility and severity of strain ageing and develop generalized models to evaluate the magnitude of the strain ageing effects on the reinforcement properties.

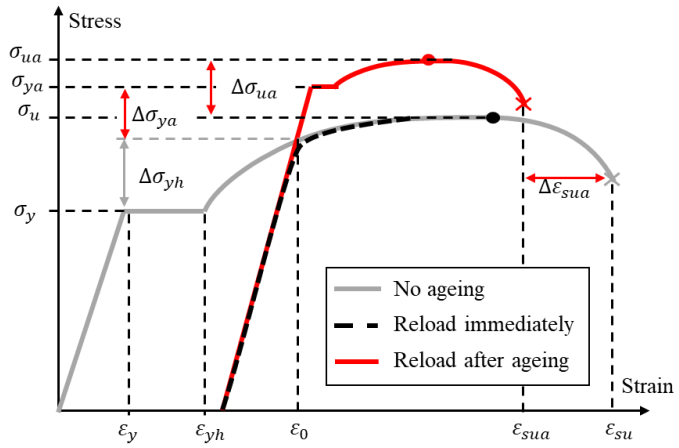

Figure 1: Effects of strain ageing on reinforcement mechanical properties.

2 QUATIFYING CHANGES IN REINFORCEMENT PROPERTIES

In this paper, the effects of strain ageing will be evaluated with respect to the reinforcement yield stress (σ_y), ultimate stress (σ_u) and fracture strain (ε_{su}) (hereon collectively referred to as 'reinforcement properties'). To enable a quantitative discussion on the change in these reinforcement properties, β-indices are defined in Equations 1-3, and representing the change with respect to the original (i.e. not strain aged) reinforcement properties. All variables are as defined in Figure 1. It is noted that the increase in yield stress (β_y) considers the increase due to strain ageing effects only (i.e., excluding strain hardening effects).

$$\beta_y = \frac{\Delta\sigma_{ya}}{\alpha_y} \tag{1}$$

$$\beta_u = \frac{\Delta\sigma_{ua}}{\sigma_u} \tag{2}$$

$$\beta_{su} = \frac{\Delta\varepsilon_{sua}}{\varepsilon_{su}} \geq \frac{\varepsilon_0 - \varepsilon_{su}}{\varepsilon_{su}} \tag{3}$$

Where, $\Delta\sigma_{ya} = \sigma_{ya} - \sigma_y$, $\Delta\sigma_{ua} = \sigma_{ua} - \sigma_u$, and $\Delta\varepsilon_{sua} = \varepsilon_{sua} - \varepsilon_{su}$. It is noted that absolute value of $\Delta\varepsilon_{sua}$ cannot exceed $\varepsilon_{su} - \varepsilon_0$.

3 EXPERIMENTAL OUTLINE

To understand the reinforcement and loading characteristics affecting strain ageing effects, an experiment was conducted on several reinforcement types. The test consisted of two series. The list reinforcement types considered for the first series is shown in the first two columns of Table 1. The test parameters considered in the second test series are shown in Table 2. The objective of the first test series was to identify the reinforcement grades susceptible to strain ageing, and the corresponding governing parameters. The test parameters for the first series were the reinforcement grade (four readily available Japanese reinforcement grades: SD295, SD345, SD395 and SD460) and reinforcement diameter (D13-D32). For each reinforcement type, the initial tensile strain, ε_0, and ageing period, t_a, were set to 3% and one year, respectively. The initial tensile strain was set to 3% to ensure the reinforcement enters the strain hardening region (i.e. yields along the full length), while the ageing period of one year was selected to simulate a fully strain aged condition (Hundy, 1954; Loporcaro, 2017; Pussegoda, 1978). The objective of the second test series was to identify the effect of the magnitude of initial tensile strain and ageing period on the magnitude of strain ageing effects. The same reinforcement type was consistently used for all tests in the second test series was (SD345, D19).

The test procedure for each test piece consisted of first subjecting it to a predetermined initial tensile strain, ε_0; ageing the reinforcement over a set ageing time period, t_a, and reloading the reinforcement in tension until fracture. The ageing time period was accelerated by heat treating the reinforcement in temperature-controlled oven (Hundy, 1954). Additional reinforcement was tensile tested directly to fracture without allowing for an ageing period. Data from these tests were used to determine σ_u and ε_{su} in Figure 1. Strain was measured as an average two strain gauges attached to reinforcement, while stress was calculated using force measured from the tensile machine. Fracture strain determined by comparing the distance between two punch marks on the reinforcement, before and after loading.

3.1 Material properties

The chemical composition of the steel for the main compounds that influence strain ageing (carbon, vanadium) (Hundy, 1954) are shown in Table 1. While nitrogen can also act as a solute atom that can lock crystal lattice dislocations, its content was not quantified in this study. It can be seen that while carbon content is relatively constant above the SD295 grade steel, vanadium content tends to increase with both increasing reinforcement yield stress and diameter (SD345).

Table 1: Summary of the key reinforcement properties used in the experiment.

		Yield stress, MPa	Ultimate stress, MPa	C	Si	Mn	Ni	Cr	Mo	V
SD295	D13	335	487	0.19%	0.15%	0.73%	0.08%	0.18%	0.016%	0.007%
SD345	D13	373	545	0.25%	0.17%	0.85%	0.09%	0.23%	0.018%	0.005%
SD345	D16	389	565	0.25%	0.17%	0.86%	0.10%	0.19%	0.018%	0.008%
SD345	D19	412	562	0.24%	0.22%	0.84%	0.07%	0.34%	0.021%	0.014%
SD345	D22	393	545	0.24%	0.18%	0.81%	0.06%	0.32%	0.016%	0.013%
SD345	D25	403	566	0.24%	0.19%	0.77%	0.08%	0.48%	0.027%	0.027%
SD345	D29	405	574	0.24%	0.29%	0.86%	0.06%	0.32%	0.018%	0.016%
SD345	D32	409	588	0.25%	0.19%	0.90%	0.07%	0.29%	0.021%	0.021%
SD390	D13	454	622	0.27%	0.16%	1.01%	0.07%	0.21%	0.014%	0.026%
SD390	D19	464	611	0.24%	0.21%	0.98%	0.07%	0.41%	0.016%	0.019%
SD490	D19	555	709	0.24%	0.23%	1.25%	NA*	NA	NA	0.056%

*NA: Not reported in mill certificate.

Table 1: Summary of parameters tested the second test series (SD345, D13).

	Ageing period, t_a (days)				
	7	**30**	**90**	**180**	**360**
Initial strain, ε_0 (%)	0.5	0.5	0.5	0.5	0.5
	1	1	1	1	1
	2	2	2	2	2
	4	4	4	4	4
	8	8	8	8	8

4 EXPERIMENTAL RESULTS

4.1 Test series 1

4.1.1 Stress-strain relationships

Representative stress-strain curves for each grade of reinforcement are shown in Figure 2. For each figure, three curves are displayed: (i) loading to fracture with no ageing (grey line), (ii) loading to the initial strain of 3% and unloading (orange line) and (iii) loading to fracture after strain ageing the reinforcement for one year (red line). It can be observed that for SD295A, SD345 and SD390 reinforcement grades, there is a clear increase in yield stress relative to the control curves following the ageing period. It can also be observed that the yield plateau is re-established. On the other hand, the higher strength SD490 grade reinforcement behaves as if reloading occurred immediately after initial strain; thus, is not susceptible to strain ageing.

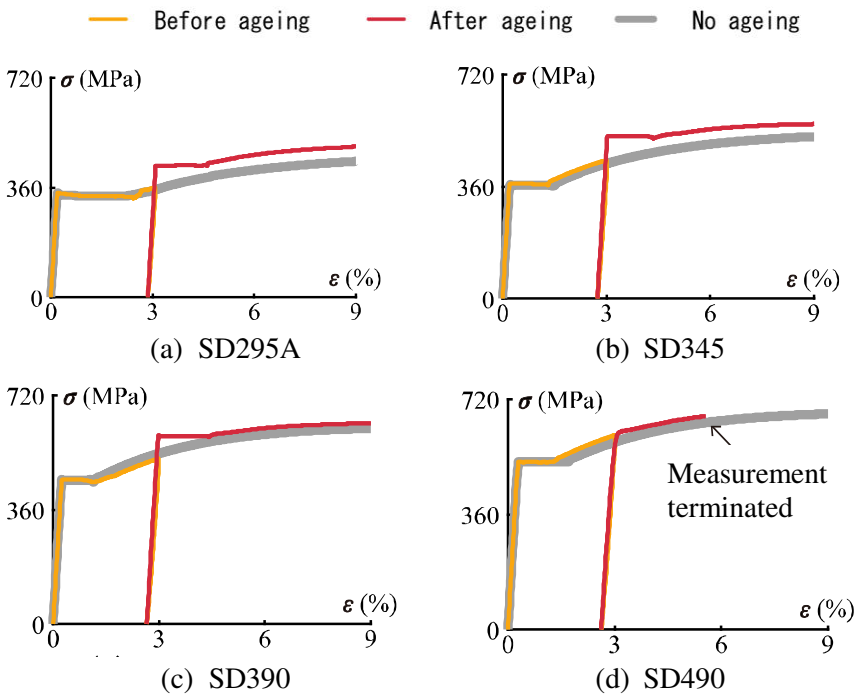

Figure 2: Representative stress-strain curves for each reinforcement grade considered in this study.

4.1.2 Relationship to chemical composition

As discussed in a previous section, the elements that are known to trigger strain ageing are carbon and nitrogen (solute atoms that migrate to and lock dislocations) while those that prevent strain ageing are

vanadium (acts to form carbine and nitride compounds, thus inhibiting the migration of solute atoms). As nitrogen content data was not available for the reinforcement, only carbon (λ_C) and vanadium contents (λ_C) are compared. The strain ageing index, β_y, is plotted against carbon content in Figure 3a. From this figure, it can be seen that the there is no clear relationship between the carbon content and β_y; thus, carbon is dismissed as a critical parameter for estimating effect of strain ageing (for the typical content found in reinforcement). On the other hand, a clear linear relationship is observed between β_y and vanadium content in Figure 3b. Specifically, the lower the vanadium content the higher the increase in yield stress due to strain ageing. At a vanadium content of 0.06% (approximately the content found in SD490 reinforcement), strain ageing effects are completely inhibited. The data in Figure 3b are approximated by a best-fit linear function expressed in Equation 4. This relationship provides a simple model for estimating the expected increase reinforcement in yield stress following one year of strain ageing, irrespective of the reinforcement grade or diameter. Similar relationships can be observed for the change in ultimate stress (β_u) and change in fracture strain (β_{su}) indices.

$$\beta_y = 0.22 - 350\lambda_v \geq 0 \tag{4}$$

$$\beta_u = 0.064 - 210\lambda_v \geq 0 \tag{5}$$

$$\beta_{su} = -0.25 + 280\lambda_v \leq 0 \tag{6}$$

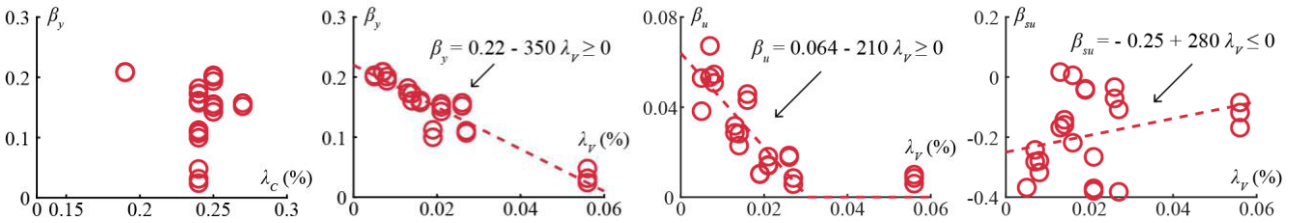

(a) β_y vs carbon content, λ_C (b) β_y vs vanadium content, λ_V (c) β_u vs vanadium content, λ_V (d) β_{su} vs vanadium content, λ_V

Figure 3: Relationship of β_y, β_u, and β_{su} with respect to carbon and vanadium content.

4.2 Test series 2

4.2.1 Stress-strain relationships

To develop a further refined prediction model for changes in reinforcement characteristics due to strain ageing, sensitivity to the initial strain and ageing period was investigated in the second test series. Representative curves for each combination of ageing time and initial strain are shown in Figure 4. It can be observed that the magnitude of yield stress increase is becomes higher as the strain ageing period becomes longer. This trend is expected as time allows for more solute atoms to migrate to lock more dislocations. The increase in yield stress is not significant for cases where the initial tensile strain was 0.5% or 1.0%. Comparatively, the increase in yield stress is higher for cases where initial strain is 2.0% or higher. It can also be observed that reinforcement subjected to initial tensile strain of 8%, and strain ageing period exceeds three months, the reinforcement necks immediately after reaching peak yield stress (i.e. brittle failure). This demonstrates the potential severity strain ageing can have on the ductility of RC structures.

4.2.2 Effect of ageing period and initial tensile strain on reinforcement properties

The change in reinforcement properties (β_y, β_u and β_{su}) with respect to ageing time, t_a, is shown in Figure 5a. It can be seen that the change in all three reinforcement properties is rapid in the first three months, but gradually slows as the strain ageing effect reaches a saturation point around the one-year mark. From a

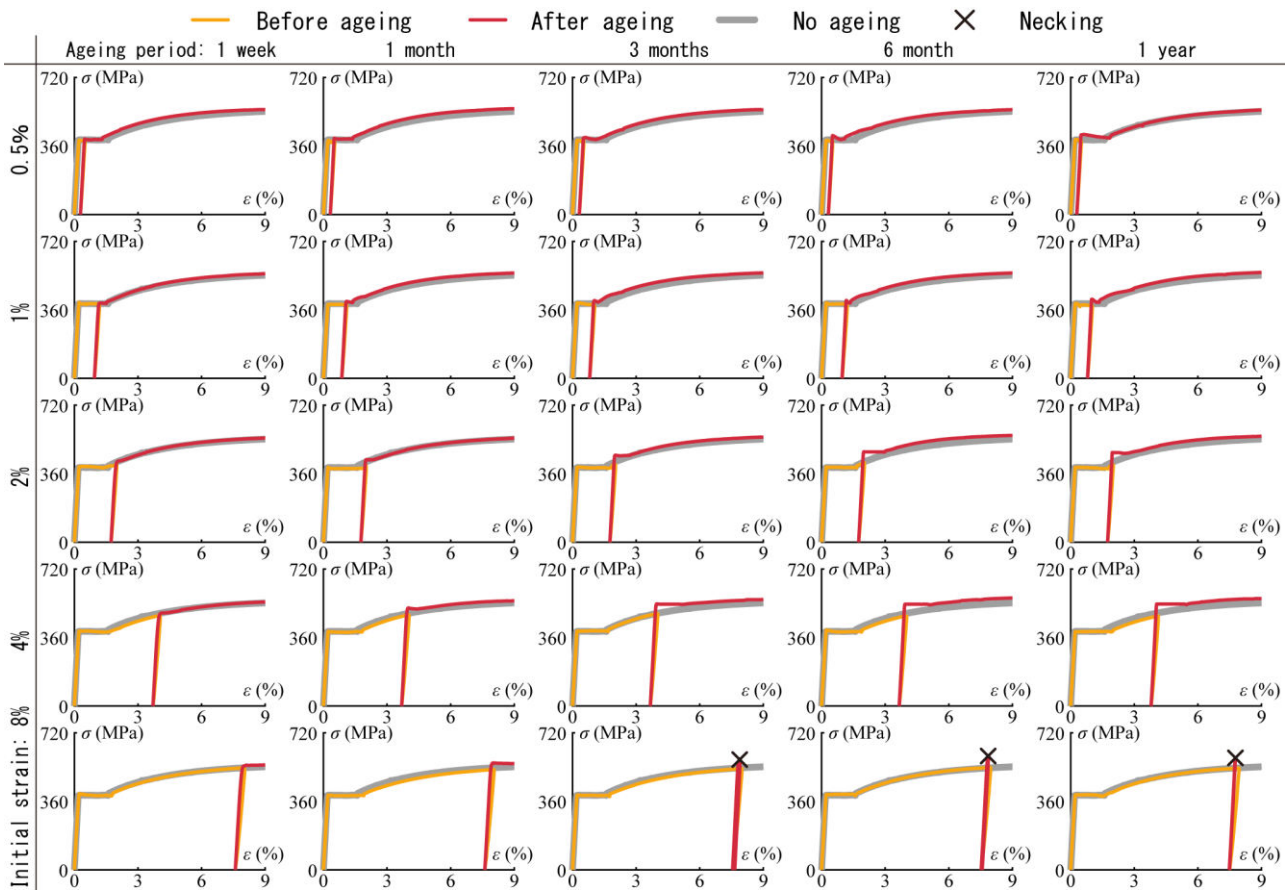

Figure 4: Representative stress-strain curves for reinforcement (SD345, D19) subjected to different initial tensile strain and ageing periods.

physical phenomenon perspective, the saturation point represents complete diffusion of solute atoms to the dislocations. For β_y , the saturation appears to happen much sooner for reinforcement subjected to initial strains below 2%. It is thought that the reason for this is that the reinforcement is not fully yielded along its length for initial strains below 2%; thus, the dislocation locations in the crystal lattice to which solute atoms can diffuse are limited, leading to earlier saturation of the strain ageing effect. Based on this, initial tensile strain corresponding to hardening strain, ε_{yh}, (i.e. strain at which strain hardening initiates) is thought to be the boundary between achieving complete and incomplete saturation of the strain ageing effect. The rate of change for reinforcement properties seen in Figure 5a can be modelled using a negative exponential relationship. Examples of such models for the experimental data of reinforcement subjected to an initial strain of $\varepsilon_0 = 8\%$ are expressed in Equations 7-9 and are plotted as dotted lines in Figure 5a.

$$\beta_y(\varepsilon_0 = 8\%) = 0.16\left(1 - e^{-\frac{t_a}{80}}\right) \tag{7}$$

$$\beta_u(\varepsilon_0 = 8\%) = 0.076\left(1 - e^{-\frac{t_a}{80}}\right) \tag{8}$$

$$\beta_{su}(\varepsilon_0 = 8\%) = -0.69\left(1 - e^{-\frac{t_a}{160}}\right) \tag{9}$$

The effect of initial strain, ε_0, on the reinforcement properties in shown in Figure 5b. First examining the β_y index, it is evident that for reinforcement subjected to an initial strain of 2% or higher, the initial strain magnitude has no effect on β_y for any given ageing period. For initial tensile strains below 2%, the trend is similar; however, the magnitude of β_y is notably lower for each ageing period compared to reinforcement

initially strained beyond 2%. This difference can similarly be attributed to the reasons of partial yielding of reinforcement described in the previous paragraph. For the β_u and β_{su} indices, reinforcement properties appear to change roughly linearly with respect to the initial strain. Examples of models for reinforcement aged for a one-year period are expressed in Equations 10-12 and are plotted as dotted lines in Figure 5b. In derivation of these equations, a constraint to meet Equations 4-6 at ε_0 = 3% was imposed.

$$\beta_y(t_a = 1y) = \begin{cases} 0.17 & for\ \varepsilon_0 > \varepsilon_{yh} \\ 0.0425 & for\ \varepsilon_0 \leq \varepsilon_{yh} \end{cases} \quad (10)$$

$$\beta_u(t_a = 1y) = -0.0025 + 1.2\varepsilon_0 \geq 0 \quad (11)$$

$$\beta_{su}(t_a = 1y) = 0.015 - 7.5\varepsilon_0 \leq 0 \quad (12)$$

Where for all cases the $\varepsilon_y \leq \varepsilon_0 \leq 0.08$ condition is imposed.

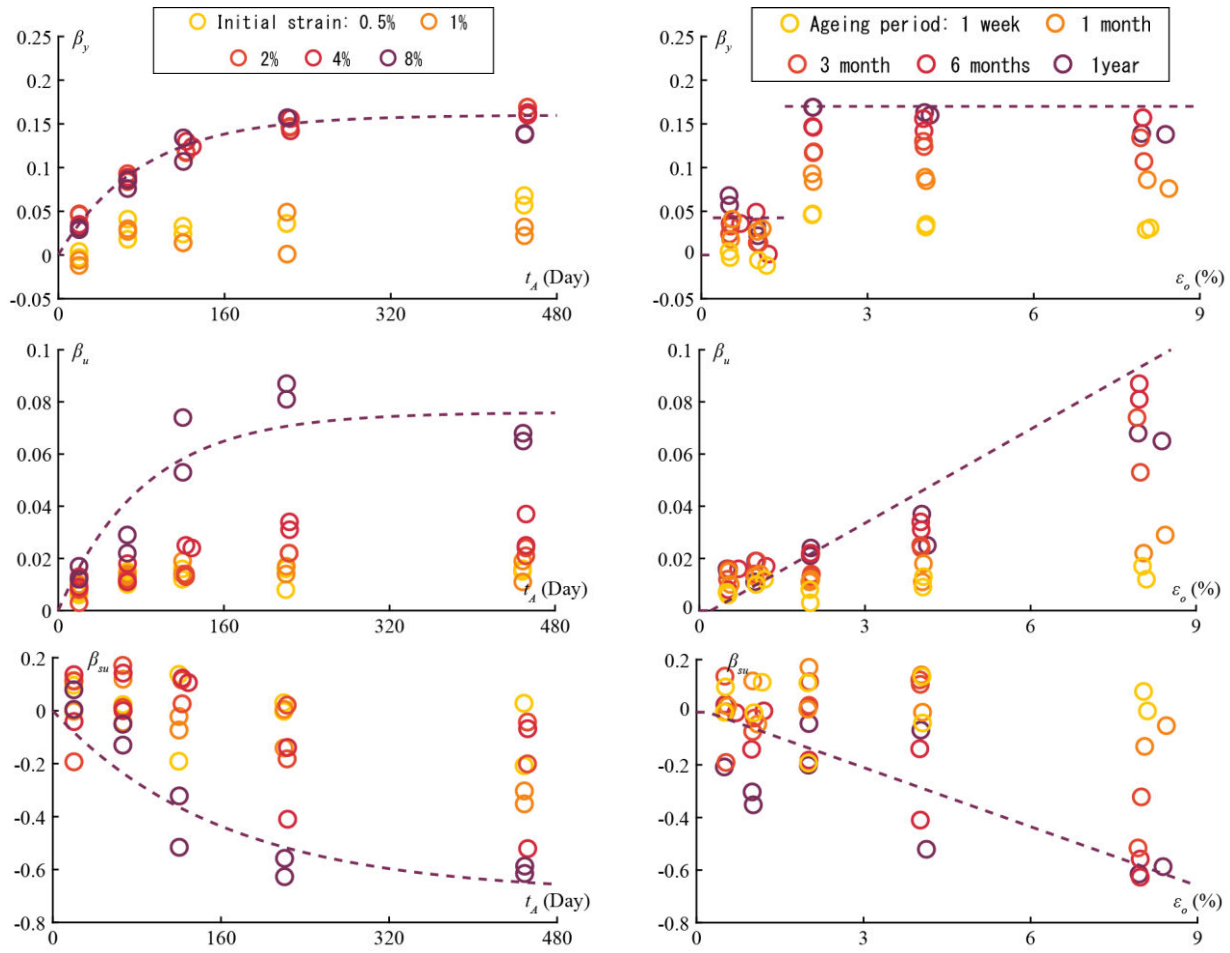

(a) Ageing period (b) Initial tensile strain

Figure 5: Effect of ageing time and initial tensile strain on reinforcement properties (β_y, β_u and β_{su}).

5 PROPOSED GENERALIZED MODEL

In Sections 3 and 4, it was demonstrated that the changes in reinforcement properties due to strain ageing is a function of vanadium content, strain ageing time and the initially applied tensile strain. In this section, these three parameters will be combined to develop an integrated expression to model the changes in reinforcement properties. A mathematical expression for the generalized model of changes of reinforcement properties due to strain ageing is proposed in Equation 13. The expression reflects the rate of strain ageing

effects via the negative exponential term (as per Section 4), while $g(\lambda_V, \varepsilon_o)$ represents the maximum expected ('saturated') change in a particular reinforcement property and is a function of vanadium content λ_V, and initial tensile strain, ε_0. The α coefficient in the negative exponential term controls the rate of convergence, and is assumed be constant for any particular reinforcement property. As in Equations 7-9, an α-value of 80, 80 and 160 is adopted for β_y, β_u and β_{su}, respectively.

$$\beta = g(\lambda_V, \varepsilon_o)\left(1 - e^{-\frac{t_a}{\alpha}}\right) \tag{13}$$

The maximum expected change for a given reinforcement characteristic, $g(\lambda_V, \varepsilon_0)$, can be calculated as a function of vanadium content using the relationships presented in Figure 3 and Equations 4-6. However, since this model was based on test data for an initial strain of 3%, it must first be normalized by the relationship to initial tensile strain (i.e. by a factor of $\beta_{su}(\varepsilon_0)/\beta_{su}(\varepsilon_0 = 3\%)$) using Equations 10-11. The resulting expressions for $g_y(\lambda_V, \varepsilon_0)$, $g_u(\lambda_V, \varepsilon_0)$ and $g_{su}(\lambda_V, \varepsilon_0)$ are presented in Equation 14-16. Adjustments for time for also implemented as the strain ageing period between the first and second test series was slightly different. Substituting Equations 14-16 into Equation 13 results in the sought generalized expressions for β_y, β_u and β_{su}, respectively.

$$g_y(\lambda_V, \varepsilon_0) = \varepsilon'_o(0.22 + 350\lambda_V) \geq 0 \qquad where\ \varepsilon'_0 = \begin{cases} 1.0 & for\ \varepsilon_0 > \varepsilon_{yh} \\ 0.25 & for\ \varepsilon_0 \leq \varepsilon_{yh} \end{cases} \tag{14}$$

$$g_u(\lambda_V, \varepsilon_0) = 29(0.064 - 210\lambda_V)(-0.0025 + 1.2\varepsilon_0) \geq 0 \tag{15}$$

$$g_{su}(\lambda_V, \varepsilon_0) = -5.4(-0.25 - 280\lambda_V)(0.015 - 7.5\varepsilon_0) \leq 0 \tag{16}$$

Where for all cases the $\varepsilon_y \leq \varepsilon_0 \leq 0.08$ condition, and limit introduced in Equations 6 are imposed.

5.1 Model validation

To examine the accuracy of the proposed model in Equations 13-16 with respect to the entire data set (test series 1 and 2), the experimentally measured (Exp.) yield stress, ultimate stress and fracture strain following strain ageing are plotted against the predicted value (Pred.) in Figure 6. For fracture strain prediction, while the general trend is captured, large scatter is observed with respect to the experimental data ($R^2 = 0.44$). The large scatter of ultimate strain prediction is attributed to the inherent inaccuracy in the method used to experimentally determine the ultimate strain described in Section 3. In comparison, yield stress and ultimate stress are both predicted to a high level of accuracy ($R^2 = 0.94$ and $R^2 = 0.99$, respectively). Limited experimental stress data obtained from strain ageing experiments in literature (Loporcaro, 2017; Pussegoda, 1978) are plotted in yellow. Results from these tests are also predicted to a high degree of accuracy, suggesting that the proposed models are reliable beyond the data of the present study.

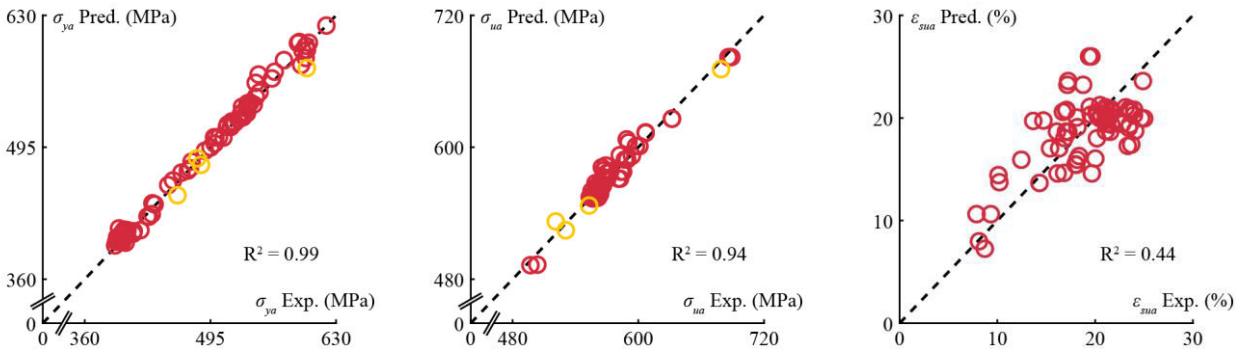

(a) Yield stress (b) Ultimate stress (d) Fracture strain

Figure 6: Verification of proposed models against experimental data.

6 CONCLUSIONS

In this study, the effects of strain ageing on reinforcement characteristics were studied through experimental testing. A large matrix of parameters was investigated to determine how various factors influence changes in reinforcement properties of yield stress, ultimate stress and fracture strain. The following conclusions are made:

1) Carbon content does not have a clear correlation with the change in reinforcement mechanical properties due to strain ageing, whereas vanadium has a clear linear relationship. Vanadium content of 0.06% seems sufficient to inhibit strain ageing effects.

2) Strain ageing effects generally increase with ageing time and saturate around one-year period mark.

3) The strain ageing effects on yield stress are independent of the initially induced strain provided that the strain exceeds the yield strain value. Reinforcement subjected to initial strains less than the hardening strain experience noticeably lower, but non-negligible strain ageing effects.

4) A model developed for predicting the magnitude of changes of reinforcement mechanical properties due to strain ageing was proposed. The model results in a moderate prediction accuracy for fracture strain (R^2 = 0.44) and high prediction accuracy for yield and ultimate stress ($R^2 \geq 0.94$).

Limited data from outside the present study was used to verify the proposed model, and only test data pertaining to monotonic loading was considered. Further tests are recommended in the future to increase confidence in the proposed models.

7 ACKNOWLEDGEMENTS

This work was supported by JSPS KAKENHI Grant Number 22K14315. Acknowledgements are also given to students of Sato-lab at Tokyo Institute of Technology who assisted in performing the experimental work.

8 REFERENCES

Hundy, B. B. (1954). Accelerated strain ageing of mild steel. *Journal of the Iron and Steel Institute*, *A*, 34–38.

Loporcaro, G. (2017). *A least invasive method to estimate the residual strain capacity of steel reinforcement in earthquake-damaged buildings* (Issue May). Ph.D Thesis. University of Canterbury.

Mikawa, A., Nagai, T., Shegay, A. V., & Maeda, M. (2022). A study on cracking behavior before and after repair of damaged RC bending fracture type seismic wall. *Annual Proceedings of the Japan Concrete Institute*, *44*(2), 271–276.

Momtahan, A., Dhakal, R. P., & Rieder, A. (2009). Effects of strain-ageing on New Zealand reinforcing steel bars. *Bulletin of the New Zealand Society for Earthquake Engineering*, *42*(3), 179–186. https://doi.org/10.5459/bnzsee.42.3.179-186

Nagai, T., Mikawa, A., Miura, K., & Maeda, M. (2022). Evaluation of recovery of seismic performance by repairing bending-yielding shear walls damaged by earthquakes. *Annual Proceedings of the Japan Concrete Institute*, *44*(2), 289–294.

Pussegoda, L. N. (1978). *Strain age embrittlement in reinforcing steels*.

Sarrafzadeh, M. (2021). *Residual Capacity and Repairability of Moderately-Damaged Ductile Reinforced Concrete Ductile Frame Structures*. PhD thesis. The University of Auckland.

Shegay, A. V, Miura, K., Akira, M., Maeda, M., & Seki, M. (2023). Performance recovery of a repaired 4-storey reinforced concrete structure subjected to shake-table testing. *Earthquake Engineering and Structural Dynamics*, 1–21. https://doi.org/https://doi.org/10.1002/eqe.3818

Tasai, A. (1988). Resistance of flexural reinforced concrete members after repair with epoxy resin. *Ninth World Conference on Earthquake Engineering*.